Conference on Modelling Fluid Flow (CMFF'18)
The 17th International Conference on Fluid Flow Technologies
Budapest, Hungary, September 4-7, 2018

DEVELOPMENT OF AIR-COOLING CONCEPTS FOR ELECTRIC MOTOR USED IN ELECTRIC AIRCRAFTS

Márton KOREN[1], Zoltán PETRÓ[2], Viktor SZENTE[3], János DOROGI[4], Gergely György BALÁZS[5]

[1] Corresponding Author. Department of Fluid Mechanics, Faculty of Mechanical Engineering, Budapest University of Technology and Economics. Bertalan Lajos u. 4 - 6, H-1111 Budapest, Hungary. Telephone: +36 30 5641993 , E-mail: koren.marci@gmail.com
[2] Corporate Technology, Siemens Zrt. Gizella u. 51 - 57, H-1143 Budapest, Hungary. , E-mail: zoltan.petro@siemens.com
[3] Department of Fluid Mechanics, Faculty of Mechanical Engineering, Budapest University of Technology and Economics. E-mail: szente@ara.bme.hu
[4] Corporate Technology, Siemens Zrt. E-mail: janos.dorogi@siemens.com
[5] Corporate Technology, Siemens Zrt. E-mail: gergely.balazs@siemens.com

ABSTRACT

Nowadays, due to the more and more important environmental issues and strict emission regulations, the electric vehicles are becoming popular and appearing in each type of transport, also in the aircraft industry. In this field, light weight, compact size, high power, and efficiency are the major design aspects. These criteria cause higher power density, thus the losses generated by the active parts are concentrated in a smaller volume. To handle the high thermal load, heat has to be effectively removed.

The aim of this article is to improve the air-cooling system of a radial flux electric motor with the help of computational fluid dynamics (CFD) simulation. The stator is cooled by a water jacket, and the rotor is cooled by air in the closed housing. Several closed concepts are examined, with the different rotor and housing geometry. During the simulations, motor with a full load at maximal rotating speed is modelled.

The results are compared with the base motor in the aspects of the critical parts' temperature, cooling performance, losses, weight, and manufacturability.

More than 40 $°C$ magnet temperature reduction can be reached with geometry modification on the housing.

Keywords: cooling, electric motor, CFD, rotor cooling, air cooled

NOMENCLATURE

P	$[W]$	power
P_l	$[W]$	loss due to fluid motion
T_c	$[°C]$	maximal coil temperature
T_m	$[°C]$	maximal magnet temperature
V	$[m^3]$	volume
f	[1]	objective function
c	[1]	coefficient of objective f.
m	$[kg]$	motor mass
q_m	$[g/s]$	mass flow rate
Δ	[1]	difference
λ	$[W/m/K]$	thermal conductivity
ρ_E	$[W/m^3]$	energy density

1. INTRODUCTION

The role of electricity as a transportation fuel is a widely investigated topic nowadays. Technology is improving, and it is starting worth it in an economical sense too. The fuel prices and the maintenance costs are much lower than for the petrol engined car, though the electric vehicle prices are higher because of the batteries. Hybrid (HEV), plug-in hybrid (PHEV), electrical (EV), and fuel cell (FCV) vehicles have been on the market since the last decade [1]. Serial produced electrical car and motorbike sells are already noticeable in the market [2]. There are electric small airplanes and motor gliders already in the production, as well [3].

There are two main ways to increase the power of an engine. The first one is to increase the efficiency. The second way is to reach the higher outcome power with increased income power. If the engine remains the same size, the power density will grow, which could be handled with higher cooling capacity. The aim of this paper to reach this greater capacity by optimizing the cooling of the electric motor, especially the rotor part.

For thermal analysis, there are several ways in the literature. The thermal equivalent circuit model or thermal network [4, 5] has the least computational cost, but it is difficult to fit the lumped convective terms, although with an accurate model good approximation can be reached, as shown by Kim and Lee [6]. The finite element (FE) models give larger spa-

tial resolution, which is necessary, where the highest temperature is critical for any parts which cannot be modelled as a lumped element [7]. The CFD could provide the most accurate solution and commonly used for optimizing parameters [8, 9], or examining effects of added extra parts [10]. Other CFD researches are specialized for a critical part of the motor, like air-gap [11, 12]. These simulation results are usually validated with measurements [8, 11, 13].

Air cooling is the simplest solution to cool the rotor. It can be open and closed type too. Pump, heat exchanger and extra sealing with additional losses are not needed, that is why this method was chosen against oil [1, 14, 15] or water cooling. And it is not dangerous, as the 70's high pressure hydrogen [16] and special materials are not needed, as for the phase change material (PCM) coolant [17]. International protection (IP) is guaranteed with closed housing.

2. CFD

Based on the 3D computer-aided design (CAD) of the electric machine, a simplified model was made. Small details, as screws, nuts, chamfers, which were neglectable for the simulation, were removed to help the meshing procedure. The total mesh numbers were more than 5 million cells. The basic mesh size is 2 *mm*, but around the smaller details, it was less. Except for the air-gap and geometrically simple parts, the mesh is unstructured. For the mesh generation, the critical parameter was the skewness value, which has to be smaller than 0.9. The mesh of the base case can be seen in 'Figure 1.'.

For simulating the rotating rotor, the moving-reference frame was used, as Jungreuthmayer et al. [13] and Kim et al. [9], which is a steady-state approach for the moving parts. It gives reasonable results, if the interference between the parts is moderate, as in this research. If it is not, mixing plane could be used, which mixing out the non-uniformity at the boundaries. Backflow could cause trouble for mixing plane models according to the Ansys manual. This

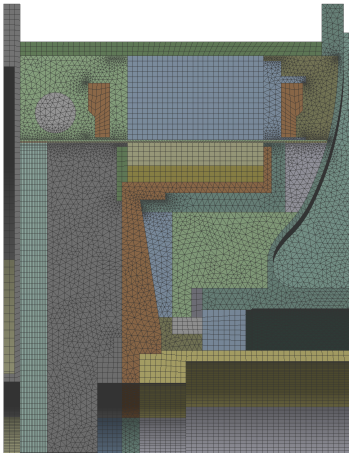

Figure 1. Mesh of the base case

Table 1. Zones

Zone Name	Material	Thermal c. $\lambda\ [W/m/K]$
Air-rotating	Air	0.0242
Air-stationary	Air	0.0242
Bearing	Steel	16.27
Housing	Aluminuim	210
Iron core-rotor	M330	42
Iron core-stator	M330	42
Magnet	NdFeB	42
Ring	Aluminuim	210
Rotor	Aluminuim	210
Screw	Steel	16.27
Shaft	42CRMO4	45.1
Spacing	Epoxy	1.2
Coil	Copper	401
Windinghead	Dupont Zytel	0.5
Wire	Copper	401

phenomenon could occur in these cases. The moving mesh methods are the closest to the reality, although the computational cost is more orders higher because the Courant number has to be guaranteed for the transient simulation. This method will be used in later stages of the motor development. During the calculations, the maximal rotating speed 2700 *rpm* was used.

The mesh in the air-gap between the rotor and the stator is critical. Here, four layers of mesh were used. Two of them belongs to the rotating frame and other two for the static one. 15 different zone was used which properties can be seen in 'Table 1.'. The inner volume was filled with air, which assumed as incompressible gas.

The computational domain was only the 1/3 of the whole motor to reduce the mesh number, although originally the rotor part was not periodic for 120°, so it had to be modified. The number of the magnets were increased in the way that the width of the plastic spacing between them remains the same. The height of these elements had to be increased, to compensate the deletion of a thin epoxy stripe, which was too small to be modelled geometrically and to reach the actual air-gap size, which was measured after manufacturing. These two modifications added up as 1.66% volume increment, which causes the same rate of energy density decreasing in the magnets. Periodic interfaces were used to connect the two ends of the model.

The windings were not modelled separately, only as a continuous body. The same method was used for the magnet elements. Thin bakelite isolations between the iron core and the windings were deleted from the geometry, like the epoxy stripe, and were modelled as a wall boundary condition. The bearings were simplified to a single ring.

The energy equation was solved for all domains. For the fluid regions, the realizable k-ϵ turbulent

Table 2. Energy sources

Part	Power P [W]	Volume V [m^3]	Energy dens. ρ_E [W/m^3]
Magnet	100	7.82E-05	4.26E+05
Iron core-r.	120	6.50E-05	6.06E+05
Iron core-s.	810	2.76E-04	9.78E+05
Coil	3790	1.91E-04	6.63E+06
Wire	38	4.59E-05	2.78E+05

model was solved, which can handle rotating element better than standard, according to Ansys Manual. The enhanced wall treatment wall function was used, which could handle a various range of $y+$ regions, by using different boundary layer equations. The difference schemes were second-order and Quick for turbulent terms, as for Kim and Lee [11].

The energy sources can be seen in 'Table 2.'. All of the heat sources were assumed as homogeneous volume source. The elements with losses had rather high heat conduction parameters, so the uniform heat source was a good approximation. The sum of them was 5 kW and these values were belonging to the maximal 55 kW motor power. This investigation was made for a medium rpm motor, which rotation speed is less than 3000 rpm, so there is no significant heat effect at the bearings.

Boundary conditions were specified as a normal environment of the motor. The ambient temperature is 25 $^\circ C$. The heat transfer coefficient is defined as 50 $W/K/m^2$ for the outer surface of the housing and the shaft. This is probably an underestimation because the motor is surrounded with high-speed turbulent air flow. The end of the shaft, which is directly connecting to the propeller, is modelled with fix temperature. The water cooling jacket around the motor is modelled with a convecting surface too, with 7000 $W/K/m^2$ heat transfer coefficient and 50 $^\circ C$ water temperature. It was assumed that the thermal contact resistance at the solid-solid interfaces and the radiation were negligible, as Kim et al. [12].

The aim of this paper to compare different concepts of the motor geometry to find an optimal cooling solution. The first model was the actual motor geometry. This case gave the main dimensions for the other concepts. The geometry of the 'Base' case can be seen at 'Fig. 2.'.

2.1. Concept 1

This concept basic idea had been given by the electromagnetic field simulations. The flux in the iron cores is not homogeneous. Low flux density part appears below the middle of the magnets/coils. And a glue-like plastic materials between the magnets are only used as fillings, as it can be seen at 'Fig. 3.'. These parts can be cut out, without disturbing strongly the electromagnetic field.

Three types of this geometry were made. 'Concept 1.2' radial blades, which increased the pressure in the back side of the engine to drive the

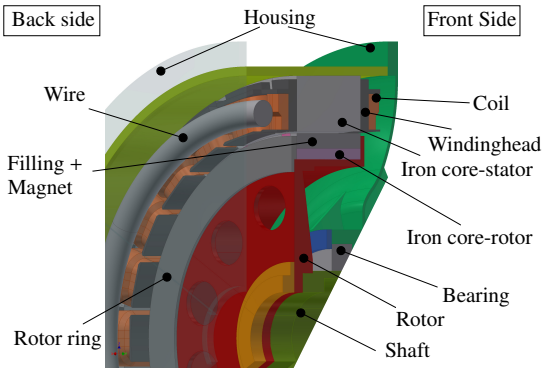

Figure 2. Base motor geometry

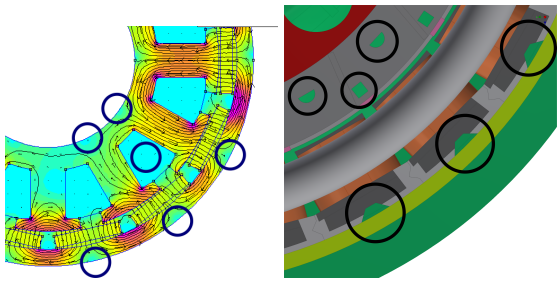

Figure 3. Holes in the electromagnetic field [18] and in the concept

airflow through the channels between the coils next to the water jacket. An extra ring was added to the back part of the housing to reduce backflow next to the back wall and drive the flow through the stator holes. On 'Concept 1.3', there are only 15 mm or 5 mm u-shape blades at the channels, which are going throw the magnet spacings. These increase the flow rate only at that channels significantly, but the torque requirements are smaller. 'Concept 1.2' was rotated in both ways. In the positive direction, the openings of the spacing channel were on the suction side of the blade row, while in the negative rotation (NR) case, the openings were in the discharge side of the blades.

2.2. Concept 2

This concept was inspired by simple electric machines to increase wall shear stresses, so the convection [13], and mix the air for the homogeneous temperature distribution. It can be reached with radial blades attached to the back side of the rotor ('Concept 2.1'). It increases the speed next to the coils and the pressure at the back side of the engine, so drive air through the gap between the coils. Increased flow speed helps the air to dissipate heat to the walls.

Instead of radial, tangential blades ('Concept 2.2') were used, which worked more as an additional cooling surface with moderate extra loss. Blades moving with high speed, which cause high heat con-

vection at the blade surfaces. Angle parameter could be optimized for this concept to increase air velocity next to the coils and still, have a moderate loss.

2.3. Concept 3

This idea was based on the fact, that the heat transfer to the water jacket was much higher, thus the inner air could be cooled by the water jacket too. Extra channel rows were added to create an airflow around the water jacket and the iron core of the rotor.

The air driving concept is the same, as 'Concept 1.2'. With radial blades pressure was increased in the back side of the engine and with a ring on the housing backflow was blocked, thus the flow went to the front part through the new channels around to the water jacket and cooled down during this, then went back to the back side through the channels under the iron cores, while it cools them down. The cross sections areas for the flows between the two side are larger than at 'Concept 1.2', so the blades can be smaller for the same flow rate.

3. RESULTS

The concepts had been compared in 'Table 3.' and can be seen graphically in 'Fig. 4'. The comparison aspects were the maximal magnet and coil temperature, hydraulic loss, mass flow rate and the mass of the motor. From these parameters, an objective function was created to compare the results quantitatively.

Table 3. Results of the simulations

Concept	Magnet t. ΔT_m [%]	Coil t. ΔT_c [%]	Loss ΔP_l [%]
Base	0.0	0.00	0
1.2	-6.6	-2.41	297
1.2 NR	-8.3	-1.86	257
1.3-15 *mm*	-5.1	0.27	68
1.3-5 *mm*	-2.8	0.69	54
2.1	-5.2	-4.47	307
2.2	-4.9	-0.82	4
3.1	-39.0	-3.23	237

Concept	Gap flow Δq_m [%]	Mass Δm [%]	Objective f. f
Base	0	0.00	0.0
1.2	79.0	-1.21	-12.3
1.2 NR	43.2	-1.21	0.0
1.3-15 *mm*	-4-7	-1.49	15.7
1.3-5 *mm*	18.2	-1.52	9.1
2.1	74.3	0.28	-24.3
2.2	-17.9	0.29	22.0
3.1	105.6	11.58	114.4

The maximal temperatures are easily accessible from the simulation results. The loss values are calculated from the torque which is acted on the rotor and the rotation speed. The mass flow rate value is the flow rate in the rotation surface only in negative y-direction because the sum of it is zero, due to the

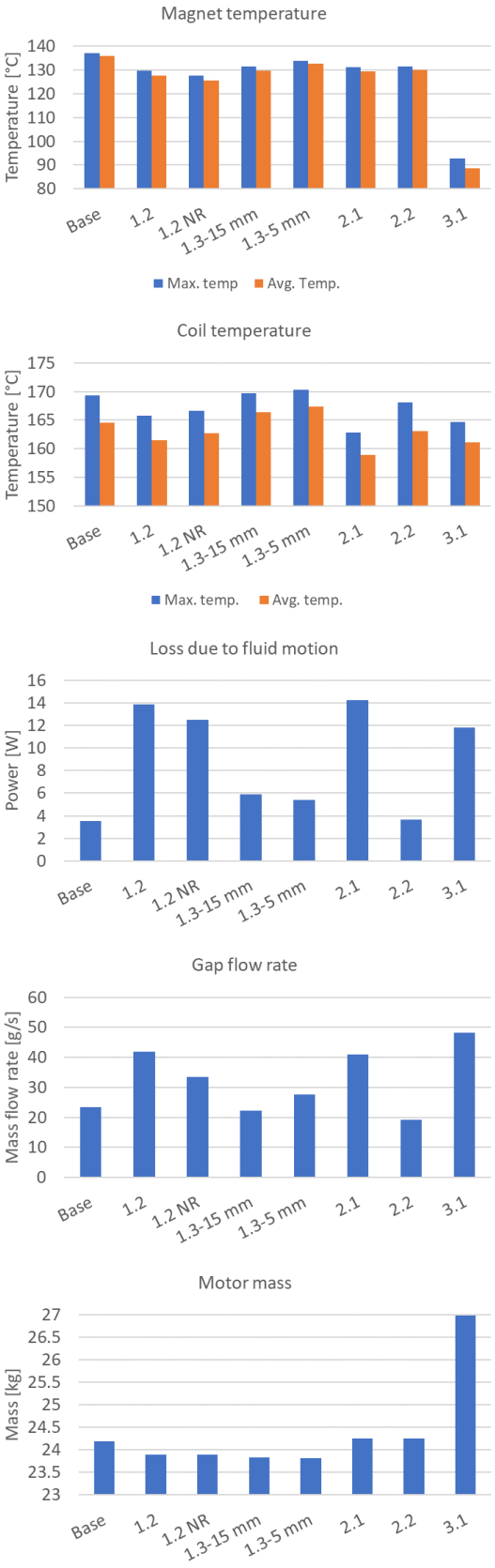

Figure 4. Results of the simulations

continuity law. The mass is the total mass of the solid parts.

The difference from the 'Base' case is calculated in percentage. For the temperature data, the basis of the percentage calculation is the difference between the ambient and the base case temperature values. These percentage values are used to calculate the objective function, which is'Eq. (1)'.

$$\begin{aligned} &\mathrm{f}(\Delta T_\mathrm{m}, \Delta T_\mathrm{c}, \Delta P_\mathrm{l}, \Delta q_m, \Delta m) = \\ &= c_1 \Delta T_\mathrm{m} + c_2 \Delta T_\mathrm{c} c_3 \Delta P_\mathrm{l} + c_4 \Delta q_m + c_5 \Delta m \end{aligned} \quad (1)$$

The coefficients of this function can be seen in 'Table 4.'. The most important aspect was the magnet temperature because overheating causes residual damages in the magnet, so this is the most critical if the power would be increased. Another important parameter is the mass. Motor for a vehicle has to be as light as possible. Lower mass means better dynamic properties. The differences are huge between the loss values, but fluid loss values are small compared to the electromagnetic losses, so this effect is compensated, with a smaller weighting coefficient. The mass flow rate is not as important than the others, and the effect of this parameter also included in the coil temperature.

Table 4. Values of the coefficient

Coeff. name	c_1	c_2	c_3	c_4	c_5
Value	-5	-1	-0.2	0.1	-3

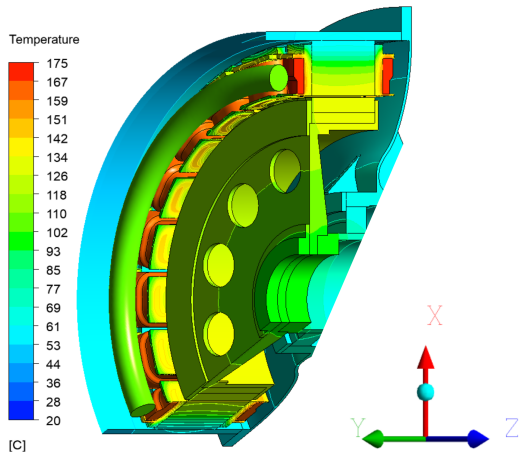

Figure 5. Temperature plot for base case

'Base' concept was the benchmark ('Fig. 5'). All cases are compared to this. The temperature scales are the same for all concepts from 25 $^\circ C$ to 170 $^\circ C$. The plots do not show the full model, bearings are masked out.

'Concept 1.2' ('Fig. 6' and 'Fig. 7') reached more than 6 % temperature decreasing for the magnet temperature in both rotating direction and there are a few percent reduction in the coils temperature

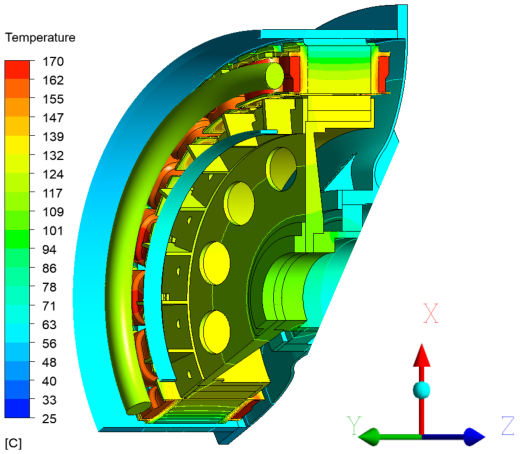

Figure 6. Temperature plot for 'Concept 1.2'

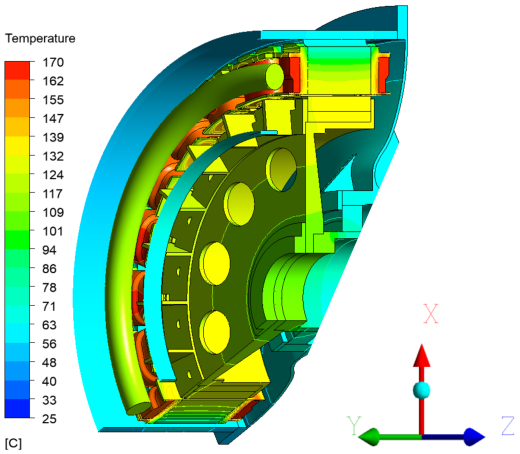

Figure 7. Temperature plot for 'Concept 1.2 NR'

too. The second phenomenon is strongly correlated with the mass flow rate values, which is significantly increased especially in the positive rotation direction way. The loss increment in the negative direction was smaller because the holes reduced the pressure peaks on the blades surfaces.

'Concept 1.3' with 15 *mm* u-shape blades ('Fig. 8') was only 1% worse for the magnets' temperature than the previous concept, although with 5 *mm* blades ('Fig. 9') the temperate reduction was the half, compared to the longer one. These blades only modified the air flow around the magnets, so the coils remained roughly at the same temperature. Loss values were a bit more than 1.5 times the original one, although less than half of 'Concept 1.2' with its large straight blades. 'Concept 1' reduces the mass of the engine. The additional blades are compensated by the holes in the spacings and in the iron cores.

'Concept 2.1' ('Fig. 10') reached 5.2% improvement for the magnets, which is the same, as the pre-

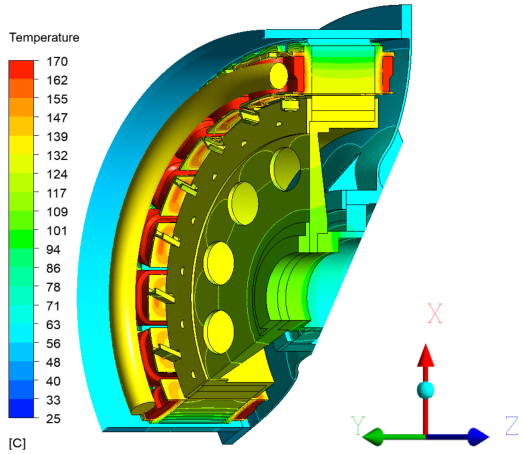

Figure 8. Temperature plot for 'Concept 1.3 15 mm'

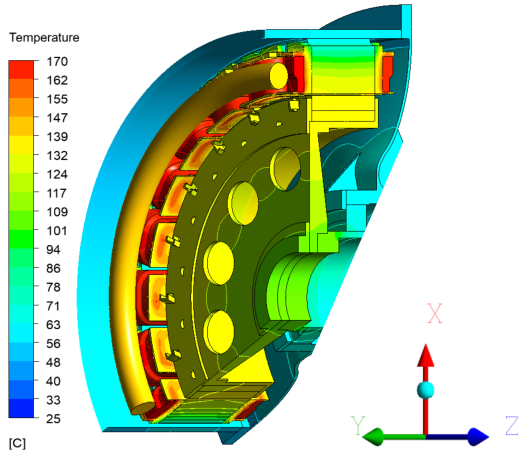

Figure 9. Temperature plot for 'Concept 1.3 5 mm'

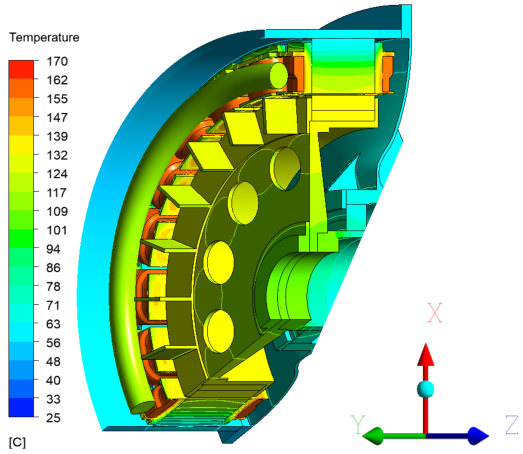

Figure 10. Temperature plot for 'Concept 2.1'

vious case with longer blades and it reached 4.7% for the coils, which caused the lowest coil temperature. The flow rate was 7/4 of the base case, that value was justified by the coil temperature reduction and the fact, that there was no any additional hole in the stator just the gaps around the coils. The drawback of this configuration was the fourth time larger loss values than the base one.

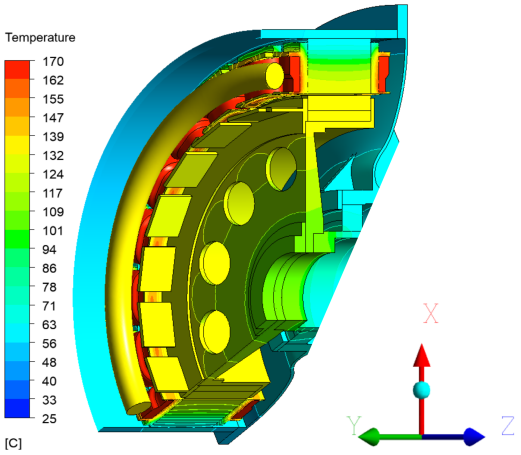

Figure 11. Temperature plot for 'Concept 2.2'

Additional loss of 'Concept 2.2' ('Fig. 11') was moderate, as it was expected. Besides this, the improvement for the magnets was only 0.3 % smaller, than for the 'Concept 2.1'. For the coils, there was no significant change, and the flow rate was even less than for the base. The blade row was perpendicular for this flow circulation direction, so probably it blocks the flow. For the two types of 'Concept 2', the mass increment can be neglected.

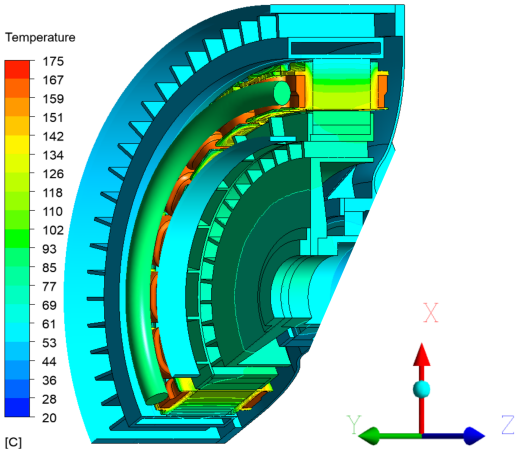

Figure 12. Temperature plot for 'Concept 3.1'

'Concept 3.1' ('Fig. 12') reached an almost 40% temperature reduction for the magnets and the loss value was still lower, that the 'Concept 1.2'. The flow ratio was more than two times the original one.

Despite this, the coil reduction was only 3.2%, which still the second largest. It shows that the flow rate was high in the additional channel rows, but beside this, it was moderate between the coils. The mass increment was 11.6 %, which is a huge drawback of this concept.

4. DISCUSSION

The electric loss is 5 kW at maximal power. Compare to this, the loss is 13.9 W due to the fluid motion in the worst case, which is about 0.3 % of the total loss. It seems small, though at high *rpm* the fluid loss remains the same, while the losses of the active part could be significantly smaller, so the ratio of the fluid loss could increase.

All of the results show, that the best one is the 'Concpet 3'. The magnet cooling capability is four times better than any other concepts. Although it has many drawbacks. First, it brakes the criteria, that the outer dimension cannot be modified. The motor mass is increasing, and the manufacturing could be more complicated compared to the other ones. Thin channel walls, as structural elements can cause mechanical problems. The water jacket cross-section area decreased, so it has to be redesigned for the smaller cross-section area and larger pressure drop, thus extra loss should be assumed.

'Concept 3' could be improved with rotor channel rows, which has a slight angel deflection from the rotation axis and could act like a fan. The row structure could be modified to decrease weight, while the cooling properties do not change significantly.

The other promising concept is the 'Concept 2.2', according to the objective function calculation. Its loss increment is moderate, but the magnet cooling ability is good. It could be easily produced because it contains only straight sheet elements.

This concept could be optimized with slightly increased angle from the tangential. Also, more blade rows could be added on both sides of the rotor. And blade shape could be changed for a bent sheet or simple wing profile.

Another further development can be to examine cases when the motor is opened to the environment, while the IP protection remains the same.

5. SUMMARY

A few concepts were introduced as an alternative electric motor geometry to reach temperature reduction of engine parts, especially for the magnets. Steady-state CFD simulations were done for 1/3 models with moving reference frame approximation. Then the simulations were compared in a quantitative way, as maximal magnet and coil temperature, loss increment due to fluid motion, mass change, volume flow values.

Magnet temperature decreased from the original 137 °C for all cases. In one case ('Concept 3.1'), the progress was even more than 44 $°C$. Although the loss due to the fluid motion was 2.4 times higher than at the original design. For this build-up, a complete redesign should have to be made.

For another concept ('Concept 2.2') 5.6 °C decreasing was reached with moderate 4.3% loss increment. This concept is easily manufacturable, and only one extra element should be added for the actual motor.

For this two concepts, further optimization should be done for the geometry. More detailed transient simulation should be for the more accurate results for the final concepts.

ACKNOWLEDGEMENTS

The authors are very grateful to Dr. Frank Anton for providing research and development directions of electric machines.

This work is related to the National Research, Development and Innovation Fund of Hungary in the frame of FIEK_16-1-2016-0007 (Higher Education and Industrial Cooperation Center) project.

REFERENCES

[1] Lee, K.-H., Cha, H.-R., and Kim, Y.-B., 2016, "Development of an interior permanent magnet motor through rotor cooling for electric vehicles", *Applied Thermal Engineering*, Vol. 95 (Supplement C), pp. 348 – 356, URL http://www.sciencedirect.com/science/article/pii/S1359431115012582.

[2] Pontes, J., 2017, "Electric Car Sales (Monthly Reports)- July", URL https://evobsession.com/electric-car-sales/, [Online; accessed 10-September-2017].

[3] wikipedia Contributors, 2017, "List of electric aircraft", URL https://en.wikipedia.org/wiki/List_of_electric_aircraft, [Online; accessed 10-September-2017].

[4] Malumbres, J. A., Satrustegui, M., Elosegui, I., Ramos, J. C., and MartÃŋnez-Iturralde, M., 2015, "Analysis of relevant aspects of thermal and hydraulic modeling of electric machines. Application in an Open Self Ventilated machine", *Applied Thermal Engineering*, Vol. 75, pp. 277 – 288, URL http://www.sciencedirect.com/science/article/pii/S1359431114008837.

[5] Kolondzovski, Z., Belahcen, A., and Arkkio, A., 2009, "Multiphysics thermal design of a high-speed permanent-magnet machine", *Applied Thermal Engineering*, Vol. 29 (13), pp. 2693 – 2700, URL http://www.sciencedirect.com/science/article/pii/S1359431109000039.

[6] Kim, C., and Lee, K.-S., 2017, "Thermal nexus model for the thermal characteristic

analysis of an open-type air-cooled induction motor", *Applied Thermal Engineering*, Vol. 112, pp. 1108 – 1116, URL http://www.sciencedirect.com/science/article/pii/S1359431116328952.

[7] Zhang, F., Song, S., Du, G., and Li, Y., 2013, "Analysis of the 3D steady temperature field of MW high speed permanent magnet motor", *2013 International Conference on Electrical Machines and Systems (ICEMS)*, pp. 1351–1354.

[8] Kim, M.-S., Lee, K.-S., and Um, S., 2009, "Numerical investigation and optimization of the thermal performance of a brushless DC motor", *International Journal of Heat and Mass Transfer*, Vol. 52 (5), pp. 1589 – 1599, URL http://www.sciencedirect.com/science/article/pii/S0017931008004821.

[9] Kim, S. C., Kim, W., and Kim, M. S., 2013, "Cooling performance of 25 kW in-wheel motor for electric vehicles", *International Journal of Automotive Technology*, Vol. 14 (4), pp. 559–567, URL https://doi.org/10.1007/s12239-013-0060-9.

[10] Streibl, B., and Neudorfer, H., 2010, "Investigating the air flow rate of self-ventilated traction motors by means of Computational Fluid Dynamics", *SPEEDAM 2010*, pp. 736–739.

[11] Kim, C., and Lee, K.-S., 2017, "Numerical investigation of the air-gap flow heating phenomena in large-capacity induction motors", *International Journal of Heat and Mass Transfer*, Vol. 110 (Supplement C), pp. 746 – 752, URL http://www.sciencedirect.com/science/article/pii/S0017931016338467.

[12] Kim, C., Lee, K.-S., and Yook, S.-J., 2016, "Effect of air-gap fans on cooling of windings in a large-capacity, high-speed induction motor", *Applied Thermal Engineering*, Vol. 100 (Supplement C), pp. 658 – 667, URL http://www.sciencedirect.com/science/article/pii/S1359431116302204.

[13] Jungreuthmayer, C., Bauml, T., Winter, O., Ganchev, M., Kapeller, H., Haumer, A., and Kral, C., 2012, "A Detailed Heat and Fluid Flow Analysis of an Internal Permanent Magnet Synchronous Machine by Means of Computational Fluid Dynamics", *IEEE Transactions on Industrial Electronics*, Vol. 59 (12), pp. 4568–4578.

[14] Gerstler, W., Ruggiero, E., Ghasripoora, F., El-Refaie, A., Bock, H. D., Shen, X., and Alexander, J., 2011, "A Liquid-Cooled Rotor for High Density Electric Machines", Vol. 47.

[15] Lim, D. H., Lee, M.-Y., Lee, H.-S., and Kim, S. C., 2014, "Performance Evaluation of an In-Wheel Motor Cooling System in an Electric Vehicle/Hybrid Electric Vehicle", Vol. 7, pp. 961–971.

[16] Armor, A. F., and Gibney, J. J., 1974, "Direct Conductor-Cooling of Large Steam Turbine-Generator 4-Pole Rotors", *IEEE Transactions on Power Apparatus and Systems*, Vol. PAS-93 (2), pp. 477–486.

[17] Wang, S., Li, Y., Li, Y.-Z., Wang, J., Xiao, X., and Guo, W., 2016, "Transient cooling effect analyses for a permanent-magnet synchronous motor with phase-change-material packaging", *Applied Thermal Engineering*, Vol. 109 (Part A), pp. 251 – 260, URL http://www.sciencedirect.com/science/article/pii/S1359431116313825.

[18] Kontkanen, T., 2016, "Perfecting BLDC performance", URL http://openservodrive.com/perfecting-bldc-performance/, [Online; accessed 02-January-2017].